Error Evaluation of Three Random Field Generators

by Gordon A. Fenton[1], Member, ASCE

Abstract

The use of multi-dimensional random fields to model real engineering systems is gaining acceptance as personal computer systems become increasingly powerful. In that the accuracy of such models depends directly on the accuracy of the algorithm used to generate realizations of the representative random fields, there is a need to evaluate and compare various random field generators. To address this issue, three common random field generators are considered in this paper; 1) the FFT method, 2) the Turning Bands Method (TBM), and 3) the Local Average Subdivision (LAS) method. For each, an ensemble of realizations of a two-dimensional homogeneous Gauss-Markov process is generated and the field mean, variance, and covariance structures are checked for statistical accuracy. Concerns such as ease of use and efficiency are also considered. It is shown that all three methods have distinct advantages and disadvantages, and the choice of algorithm will depend on the particular application. A number of guidelines and suggestions are made to help avoid or minimize problems associated with each method.

Introduction

Random field models of complex engineering systems having spatially variable properties are becoming increasingly common. This trend is motivated by the widespread acceptance of reliability methods in engineering design and is made possible by the increasing power of personal computers. It is no longer sufficient to base designs on best estimate or mean values alone. Information quantifying uncertainty and variability in the system must also be incorporated to allow the calculation of failure probabilities associated with various limit state criteria. To accomplish this, a probabilistic model is required. In that most engineering systems involve loads and materials spread over some spatial extent, their properties are appropriately represented by random fields. For example, to estimate the failure probability of a highway bridge, a designer may represent both concrete strength and input earthquake ground motion using independent random fields, the latter time varying. Subsequent analysis using a Monte Carlo approach and a dynamic finite element package would lead to the desired statistics.

In this paper, a number of different algorithms which can be used to produce scalar multi-dimensional random fields are evaluated in light of their accuracy, efficiency, ease of implementation, and ease of use. Many different random field generator algorithms are available of which the following are perhaps the most common:

1) Moving Average (MA) methods,
2) Discrete Fourier Transform (DFT) method,
3) Covariance Matrix Decomposition,

[1] Assistant Professor, Applied Mathematics, Technical University of Nova Scotia, Halifax, Nova Scotia, B3J 2X4

4) Fast Fourier Transform (FFT) method,

5) Turning Bands Method (TBM),

6) Local Average Subdivision (LAS) method,

In all of these methods, only the first two moments of the target field may be specified, namely the mean and covariance structure. Since this completely characterizes a Gaussian field, attention will be restricted in the following to such fields. (Non-Gaussian fields may be created through non-linear transformations of Gaussian fields, however some care must be taken since the mean and covariance structure will also be transformed.) In addition, only weakly homogeneous fields, whose first two moments are independent of spatial position, will be considered in this paper.

Although potentially very accurate, both the Moving Average and the DFT methods tend to be computationally slow. At each point $\underset{\sim}{x}$ in space, the MA technique constructs the random field $Z(\underset{\sim}{x})$ as a weighted average of a white noise process

$$Z(\underset{\sim}{x}) = \int_{-\infty}^{\infty} f(\underset{\sim}{\xi} - \underset{\sim}{x}) dW(\underset{\sim}{\xi}) \tag{1}$$

where $dW(\underset{\sim}{\xi})$ is a mean zero incremental white noise process with variance $d\underset{\sim}{\xi}$ and f is a weighting function. In practice (1) is computed as a sum, its extent and resolution directly affecting the accuracy of the resulting field. Because the sum is computed separately at each point $\underset{\sim}{x}$, the moving average technique can be very computationally expensive. For reasonable sized fields in two and higher dimensions it can be orders of magnitude slower than some of the other methods to be discussed. This, along with the fact that the weighting function f can be difficult to find for an arbitrary covariance structure, renders the method unwieldy in practice and it will not be considered further. In a sequence of two papers, Mignolet and Spanos (1992) and Spanos and Mignolet (1992) discuss in considerable detail the moving average (MA), autoregressive (AR) and ARMA approaches to simulating two-dimensional random fields. In their examples, they obtain accurate results at the expense of running about 10 or more times slower than the fastest of the methods to be considered here.

The Fourier Transform methods are based on the spectral representation of homogeneous mean square continuous random fields, $Z(\underset{\sim}{x})$, which can be expressed as follows (Yaglom, 1962)

$$Z(\underset{\sim}{x}) = \int_{-\infty}^{\infty} e^{i\underset{\sim}{x}\cdot\underset{\sim}{\omega}} W(d\underset{\sim}{\omega}) \tag{2}$$

where $W(d\underset{\sim}{\omega})$ is an interval white noise process with mean zero and variance $S(\underset{\sim}{\omega})d\underset{\sim}{\omega}$. This representation is in terms of the physically meaningful spectral density function, $S(\underset{\sim}{\omega})$, and so is intuitively attractive. In practice, the n-dimensional integral becomes an n-dimensional sum. In the case of the Discrete Fourier Transform, the sum is evaluated separately at each point $\underset{\sim}{x}$ which, although potentially accurate, is computationally slow for reasonable field sizes and typical spectral density functions – the DFT is generally about as efficient as the MA discussed above. Its major advantage over the MA approach is that the spectral density function is estimated in practice using standard techniques. However, because of its inefficiency, the DFT approach will not be considered further in this paper.

Covariance matrix decomposition is a direct method of producing a homogeneous random field with prescribed covariance structure $B(\underset{\sim}{x}_i - \underset{\sim}{x}_j) = B(\underset{\sim}{\tau}_{ij})$, where $\underset{\sim}{x}_i$, $i = 1, 2, \ldots, n$ are discrete

points in the field and $\underset{\sim}{\tau}_{ij}$ is the lag vector between the points $\underset{\sim}{x}_i$ and $\underset{\sim}{x}_j$. If $\underset{\approx}{B}$ is a positive definite covariance matrix with elements $B_{ij} = B(\underset{\sim}{\tau}_{ij})$, then a mean zero discrete process $Z_i = Z(\underset{\sim}{x}_i)$ can be produced (using vector notation) according to

$$\underset{\sim}{Z} = \underset{\approx}{L}\,\underset{\sim}{U} \tag{3}$$

where $\underset{\approx}{L}$ is a lower triangular matrix satisfying $\underset{\approx}{L}\underset{\approx}{L}^T = \underset{\approx}{B}$ (typically obtained using Cholesky decomposition) and $\underset{\sim}{U}$ is a vector of n independent mean zero, unit variance Gaussian random variables. Although appealing in its simplicity and accuracy, this method is only useful for small fields. In two dimensions, the covariance matrix of a 128×128 field would be of size $16,384 \times 16,384$ and the Cholesky decomposition of such a matrix would be both time consuming and prone to considerable round-off error.

In the remainder of the paper, attention will be focused on the last three methods mentioned above, namely the Fast Fourier Transform (FFT), the Turning Bands Method (TBM), and the Local Average Subdivision (LAS) algorithms. Some of the discussion will be based on observations of simulations, which in all cases will be of a homogeneous isotropic Gaussian random field with Gauss-Markov covariance structure

$$B(\underset{\sim}{\tau}) = \sigma^2\, e^{-2|\underset{\sim}{\tau}|/\theta} \tag{4}$$

where σ^2 is the variance of the process (in this case unity), and θ is the scale of fluctuation. Reference will be made to the estimated mean and variance fields which are simply the mean and variance estimated at each field point over an ensemble of realizations. At each point in the field, the mean and variance are expected to follow that predicted by theory for random samples of a Gaussian process and the fields are inspected for the presence of patterns indicating errors and/or bias.

The FFT, TBM and LAS methods are typically much more efficient than the first three methods discussed above. However, the gains in efficiency do not come without some loss in accuracy, as is typical in numerical methods. In the next few sections, the paper proposes an implementation strategy for the FFT method and reviews the TBM and LAS methods. The types of errors associated with each method and ways to avoid them will be discussed in some detail. Finally the methods will be compared and guidelines as to their use suggested.

The Fast Fourier Transform Method

In order to apply the Fast Fourier Transform method (see, for example, Cooley and Tukey, 1965) to compute Eq. (2), a number of additional assumptions are needed. First, the process $Z(\underset{\sim}{x})$ is assumed to be mean zero, real and discrete. For the purposes of this development, only the one-dimensional case will be considered and multi-dimensional results will be stated subsequently. For discrete $Z(x_j)$, $j = 1, 2, \ldots, N$, Eq. (2) becomes

$$\begin{aligned} Z(x_j) &= \int_{-\pi}^{\pi} e^{ix_j\omega}\, W(d\omega) \\ &= \lim_{K\to\infty} \sum_{k=-K}^{K} e^{ix_j\omega_k}\, W(\Delta\omega_k) \end{aligned}$$

$$= \lim_{K\to\infty} \sum_{k=-K}^{K} \left\{ \mathcal{A}(\Delta\omega_k)\cos(x_j\omega_k) + \mathcal{B}(\Delta\omega_k)\sin(x_j\omega_k) \right\} \tag{5}$$

where $\omega_k = k\pi/K$, $\Delta\omega_k$ is an interval of length π/K centered at ω_k, and the last step in (5) follows from the fact that Z is real. The functions $\mathcal{A}(\Delta\omega_k)$ and $\mathcal{B}(\Delta\omega_k)$ are independent identically distributed random interval functions with mean zero and E $[\mathcal{A}(\Delta\omega_k)\mathcal{A}(\Delta\omega_m)]$ = E $[\mathcal{B}(\Delta\omega_k)\mathcal{B}(\Delta\omega_m)]$ = 0 for all $k \neq m$ in the limit as $\Delta\omega \to 0$. At this point, the simulation involves generating realizations of $\mathcal{A}_k = \mathcal{A}(\Delta\omega_k)$ and $\mathcal{B}_k = \mathcal{B}(\Delta\omega_k)$ and evaluating (5). Since the process is real, $S(\omega) = S(-\omega)$, and the variances of $\mathcal{A}_k$ and $\mathcal{B}_k$ can be expressed in terms of the one-sided spectral density function $G(\omega) = 2S(\omega)$, $\omega \geq 0$. This means that the sum in (5) can have lower bound $k = 0$. Note that an equivalent way of writing (5) is

$$Z(x_j) = \sum_{k=0}^{K} \mathcal{C}_k \cos(x_j\omega_k + \Phi_k), \tag{6}$$

where Φ_k is a random phase angle uniformly distributed on $[0, 2\pi]$ and $\mathcal{C}_k$ follows a Rayleigh distribution. Shinozuka and Jan (1972) take $\mathcal{C}_k = \sqrt{2G(\omega_k)\Delta\omega}$ to be deterministic, an approach not followed here since it gives an upper bound on Z over the space of outcomes of $Z \leq \sum_{k=0}^{K} \sqrt{2G(\omega_k)\Delta\omega}$ which may be an unrealistic restriction, particularly in reliability calculations.

Next, the process $Z_j = Z(x_j)$ is assumed to be periodic, $Z_j = Z_{K+j}$, with the same number of spatial and frequency discretization points ($N = K$). As will be shown later, the periodicity assumption leads to a symmetric covariance structure which is perhaps the major disadvantage to the FFT approach. If the physical length of the one-dimensional process under consideration is D and the space and frequency domains are discretized according to

$$x_j = j\Delta x = \frac{jD}{K-1} \tag{7}$$

$$\omega_j = j\Delta\omega = \frac{2\pi j(K-1)}{KD} \tag{8}$$

for $j = 0, 1, \ldots, K-1$, then the Fourier transform

$$Z_j = \sum_{k=0}^{K-1} \mathcal{X}_k e^{i(2\pi jk/K)} \tag{9}$$

can be evaluated using the FFT algorithm. The Fourier coefficients, $\mathcal{X}_k = \mathcal{A}_k - i\mathcal{B}_k$, have the following symmetries due to the fact that Z is real,

$$\mathcal{A}_k = \frac{1}{K} \sum_{j=0}^{K-1} Z_j \cos 2\pi \tfrac{jk}{K} = \mathcal{A}_{K-k} \tag{10}$$

$$\mathcal{B}_k = \frac{1}{K} \sum_{j=0}^{K-1} Z_j \sin 2\pi \tfrac{jk}{K} = -\mathcal{B}_{K-k} \tag{11}$$

which means that $\mathcal{A}_k$ and $\mathcal{B}_k$ need only be generated randomly for $k = 0, 1, \ldots, K/2$ and that $\mathcal{B}_0 = \mathcal{B}_{K/2} = 0$. Note that if the coefficients at $K-k$ are produced independently of the coefficients

at k, the resulting field will display aliasing. Thus there is no advantage to taking Z to be complex, generating all the Fourier coefficients randomly, and attempting to produce two independent fields simultaneously (the real and imaginary parts), or in just ignoring the imaginary part.

As far as the simulation is concerned, all that remains is to specify the statistics of $\mathcal{A}_k$ and $\mathcal{B}_k$ so that they can be generated randomly. If Z is a Gaussian mean zero process, then so are $\mathcal{A}_k$ and $\mathcal{B}_k$. The variance of $\mathcal{A}_k$ can be computed in a consistent fashion (Fenton, 1990) by evaluating $\mathrm{E}\left[\mathcal{A}_k^2\right]$ using (10)

$$\mathrm{E}\left[\mathcal{A}_k^2\right] = \frac{1}{K^2}\sum_{j=0}^{K-1}\sum_{\ell=0}^{K-1}\mathrm{E}\left[Z_j\,Z_\ell\right]\cos 2\pi\tfrac{jk}{K}\cos 2\pi\tfrac{\ell k}{K} \tag{12}$$

This result suggests using the covariance function directly to evaluate the variance of $\mathcal{A}_k$, an approach that was investigated by Fenton (1990), however the implementation is complex and no particular advantage in accuracy was noticed. A simpler approach involves the discrete approximation to the Wiener-Khinchine relationship

$$\mathrm{E}\left[Z_j\,Z_\ell\right] \simeq \Delta\omega\sum_{m=0}^{K-1} G(\omega_m)\cos 2\pi\tfrac{m(j-\ell)}{K} \tag{13}$$

which when substituted into (12) leads to

$$\begin{aligned}\mathrm{E}\left[\mathcal{A}_k^2\right] &= \frac{\Delta\omega}{K^2}\sum_{j=0}^{K-1}\sum_{\ell=0}^{K-1}\sum_{m=0}^{K-1} G(\omega_m)\cos 2\pi\tfrac{m(j-\ell)}{K}C_{kj}C_{k\ell}\\ &= \frac{\Delta\omega}{K^2}\sum_{m=0}^{K-1} G(\omega_m)\sum_{j=0}^{K-1} C_{mj}C_{kj}\sum_{\ell=0}^{K-1} C_{m\ell}C_{k\ell}\\ &+ \frac{\Delta\omega}{K^2}\sum_{m=0}^{K-1} G(\omega_m)\sum_{j=0}^{K-1} S_{mj}C_{kj}\sum_{\ell=0}^{K-1} S_{m\ell}C_{k\ell},\end{aligned} \tag{14}$$

where $C_{kj} = \cos 2\pi\frac{kj}{K}$ and $S_{kj} = \sin 2\pi\frac{kj}{K}$.

To reduce (14) further, use is made of the following two identities

1) $$\sum_{k=0}^{K-1}\sin 2\pi\tfrac{mk}{K}\cos 2\pi\tfrac{jk}{K} = 0$$

2) $$\sum_{k=0}^{K-1}\cos 2\pi\tfrac{mk}{K}\cos 2\pi\tfrac{jk}{K} = \begin{cases} 0, & \text{if } m \neq j\\ \frac{K}{2}, & \text{if } m = j \text{ or } K-j\\ K, & \text{if } m = j = 0 \text{ or } \frac{K}{2}\end{cases}$$

By identity (1), the second term of (14) is zero. The first term is also zero, except when $m = k$ or $m = K - k$, leading to the results

$$\mathrm{E}\left[\mathcal{A}_k^2\right] = \begin{cases}\frac{1}{2}G(\omega_k)\Delta\omega, & \text{if } k = 0\\ \frac{1}{4}\{G(\omega_k) + G(\omega_{K-k})\}\Delta\omega, & \text{if } k = 1,\ldots,\frac{K}{2}-1\\ G(\omega_k)\Delta\omega, & \text{if } k = \frac{K}{2}\end{cases} \tag{15}$$

remembering that for $k = 0$ the frequency interval is $\frac{1}{2}\Delta\omega$. An entirely similar calculation leads to

$$\mathrm{E}\,[\mathcal{B}_k]^2 = \begin{cases} 0, & \text{if } k = 0 \text{ or } \frac{K}{2} \\ \frac{1}{4}\{G(\omega_k) + G(\omega_{K-k})\}\Delta\omega, & \text{if } k = 1, \ldots, \frac{K}{2} - 1 \end{cases} \tag{16}$$

Thus the simulation process is as follows;

1) generate independent normally distributed realizations of $\mathcal{A}_k$ and $\mathcal{B}_k$ having mean zero and variance given by (15) and (16) for $k = 0, 1, \ldots, K/2$ and set $\mathcal{B}_0 = \mathcal{B}_{K/2} = 0$,
2) use the symmetry relationships, (10) and (11), to produce the remaining Fourier coefficients for $k = 1 + K/2, \ldots, K - 1$
3) produce the field realization by Fast Fourier Transform using Eq. (9).

In higher dimensions a similar approach can be taken. To compute the Fourier sum over non-negative frequencies only, the spectral density function $S(\underset{\sim}{\omega})$ is assumed to be even in all components of $\underset{\sim}{\omega}$ (quadrant symmetric) so that the 'one-sided' spectral density function, $G(\underset{\sim}{\omega}) = 4S(\underset{\sim}{\omega})\,\forall\ \omega_i \geq 0$, can be employed. Using $L = K_1 - \ell$, $M = K_2 - m$, and $N = K_3 - n$ to denote the symmetric points in fields of size $K_1 \times K_2$ in 2-D or $K_1 \times K_2 \times K_3$ in 3-D, the Fourier coefficients yielding a real two-dimensional process must satisfy

$$\begin{aligned} \mathcal{A}_{LM} &= \mathcal{A}_{\ell m}, & \mathcal{B}_{LM} &= -\mathcal{B}_{\ell m} \\ \mathcal{A}_{\ell M} &= \mathcal{A}_{L m}, & \mathcal{B}_{\ell M} &= -\mathcal{B}_{L m} \end{aligned} \tag{17}$$

for $\ell, m = 0, 1, \ldots, \frac{K_\alpha}{2}$ where K_α is either K_1 or K_2 appropriately. Note that these relationships are applied modulo K_α, so that $\mathcal{A}_{K_1-0,m} \equiv \mathcal{A}_{0,m}$ for example. In two dimensions, the Fourier coefficients must be generated over two adjacent quadrants of the field, the rest of the coefficients obtained using the symmetry relations. In three dimensions, the symmetry relationships are

$$\begin{aligned} \mathcal{A}_{LMN} &= \mathcal{A}_{\ell mn}, & \mathcal{B}_{LMN} &= -\mathcal{B}_{\ell mn} \\ \mathcal{A}_{\ell MN} &= \mathcal{A}_{L mn}, & \mathcal{B}_{\ell MN} &= -\mathcal{B}_{L mn} \\ \mathcal{A}_{L mN} &= \mathcal{A}_{\ell M n}, & \mathcal{B}_{L mN} &= -\mathcal{B}_{\ell M n} \\ \mathcal{A}_{\ell mN} &= \mathcal{A}_{LMn}, & \mathcal{B}_{\ell mN} &= -\mathcal{B}_{LMn} \end{aligned} \tag{18}$$

for $\ell, m, n = 0, 1, \ldots, \frac{K_\alpha}{2}$. Again, only half the Fourier coefficients are to be generated randomly.

The variances of the Fourier coefficients are found in a manner analogous to the one-dimensional case, resulting in

$$\mathrm{E}\,\left[\mathcal{A}^2_{\ell m}\right] = \tfrac{1}{8}\delta^A_{\ell m}\Delta\underset{\sim}{\omega}\left(G^d_{\ell m} + G^d_{\ell N} + G^d_{L n} + G^d_{LN}\right) \tag{19}$$

$$\mathrm{E}\,\left[\mathcal{B}^2_{\ell m}\right] = \tfrac{1}{8}\delta^B_{\ell m}\Delta\underset{\sim}{\omega}\left(G^d_{\ell m} + G^d_{\ell N} + G^d_{L n} + G^d_{LN}\right) \tag{20}$$

for two-dimensions and

$$\mathrm{E}\,[\mathcal{A}_{\ell mn}]^2 = \tfrac{1}{16}\delta^A_{\ell mn}\Delta\underset{\sim}{\omega}\left(G^d_{\ell mn} + G^d_{\ell mN} + G^d_{\ell Mn} + G^d_{Lmn} + G^d_{\ell MN} + G^d_{LmN} + G^d_{LMn} + G^d_{LMN}\right) \tag{21}$$

$$\mathrm{E}\,[\mathcal{B}_{\ell mn}]^2 = \tfrac{1}{16}\delta^B_{\ell mn}\Delta\underset{\sim}{\omega}\left(G^d_{\ell mn} + G^d_{\ell mN} + G^d_{\ell Mn} + G^d_{Lmn} + G^d_{\ell MN} + G^d_{LmN} + G^d_{LMn} + G^d_{LMN}\right) \tag{22}$$

in three-dimensions, where for p dimensions,

$$\Delta\underset{\sim}{\omega} = \prod_{i=1}^{p} \Delta\omega_i, \tag{23}$$

$$G^d(\underset{\sim}{\omega}) = \frac{G(\omega_1, \ldots, \omega_p)}{2^d}, \tag{24}$$

and d is the number of components of $\underset{\sim}{\omega} = (\omega_1, \ldots, \omega_p)$ which are equal to zero. The factors $\delta^A_{\ell mn}$ and $\delta^B_{\ell mn}$ are given by

$$\delta^A_{\ell mn} = \begin{cases} 2 & \text{if } \ell = 0 \text{ or } \frac{K_1}{2} \text{ and } m = 0 \text{ or } \frac{K_2}{2} \text{ and } n = 0 \text{ or } \frac{K_3}{2} \\ 1 & \text{otherwise} \end{cases} \tag{25}$$

$$\delta^B_{\ell mn} = \begin{cases} 0 & \text{if } \ell = 0 \text{ or } \frac{K_1}{2} \text{ and } m = 0 \text{ or } \frac{K_2}{2} \text{ and } n = 0 \text{ or } \frac{K_3}{2} \\ 1 & \text{otherwise} \end{cases} \tag{26}$$

(ignoring the index n in the case of two dimensions). Thus, in higher dimensions, the simulation procedure is almost identical to that followed in the 1-D case – the only difference being that the coefficients are generated randomly over the half plane (2-D) or the half volume (3-D) rather than the half line of the 1-D formulation.

It is appropriate at this time to investigate some of the shortcomings of the method. First of all it is easy to show that regardless of the desired target covariance function, the covariance function $\hat{B}_k = \hat{B}(k\Delta x)$ of the real FFT process is always symmetric about the midpoint of the field. In one-dimension, the covariance function is given by (using complex notation for the time being),

$$\begin{aligned} \hat{B}_k &= \mathrm{E}\left[Z_{\ell+k}\overline{Z_\ell}\right] \\ &= \mathrm{E}\left[\sum_{j=0}^{K-1} \mathcal{X}_j \exp\left\{i\left(\tfrac{2\pi(\ell+k)j}{K}\right)\right\} \sum_{m=0}^{K-1} \overline{\mathcal{X}_m} \exp\left\{-i\left(\tfrac{2\pi\ell m}{K}\right)\right\}\right] \\ &= \sum_{j=0}^{K-1} \mathrm{E}\left[\mathcal{X}_j\overline{\mathcal{X}_j}\right] \exp\left\{i\left(\tfrac{2\pi jk}{K}\right)\right\}, \end{aligned} \tag{27}$$

where use was made of the fact that $\mathrm{E}\left[\mathcal{X}_j\overline{\mathcal{X}_m}\right] = 0$ for $j \neq m$ (overbar denotes the complex conjugate). Similarly one can derive

$$\begin{aligned} \hat{B}_{K-k} &= \sum_{j=0}^{K-1} \mathrm{E}\left[\mathcal{X}_j\overline{\mathcal{X}_j}\right] \exp\left\{-i\left(\tfrac{2\pi jk}{K}\right)\right\} \\ &= \overline{\hat{B}_k} \end{aligned} \tag{28}$$

since $\mathrm{E}\left[\mathcal{X}_j\overline{\mathcal{X}_j}\right]$ is real. The covariance function of a real process is also real in which case (28) becomes simply

$$\hat{B}_{K-k} = \hat{B}_k. \tag{29}$$

In one dimension, this symmetry is illustrated by Figure 1. Similar results are observed in higher dimensions. In general, this deficiency can be overcome by generating a field twice as long as required in each coordinate direction and keeping only the first quadrant of the field. Figure 1 also compares the covariance, mean, and variance fields of the LAS method to that of the FFT method (the TBM method is not defined in one dimension). The two methods give satisfactory performance with respect to the variance and mean fields, while the LAS method shows superior performance with respect to the covariance structure.

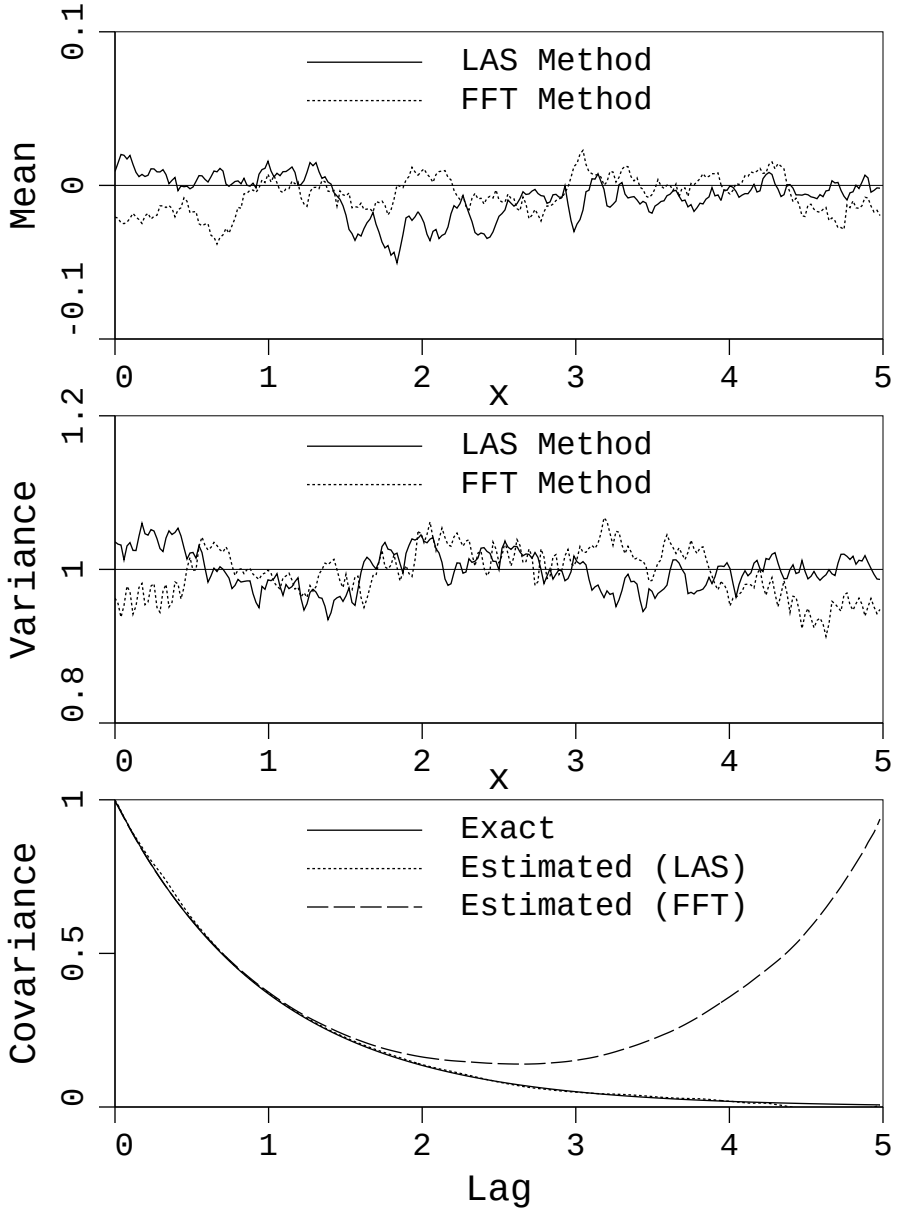

Figure 1. Mean, variance, and covariance of a 1-D 128 point Gauss-Markov process estimated over an ensemble of 2000 realizations.

The second problem with the FFT method relates primarily to its ease of use. Because of the close relationship between the spatial and frequency discretization, considerable care must be exercised when initially defining the spatial field and its discretization. First of all the physical length of the field D must be large enough that the frequency increment $\Delta\omega = 2\pi(K-1)/KD \simeq 2\pi/D$ is sufficiently small. This is necessary if the sequence $\frac{1}{2}G(\omega_0)\Delta\omega, G(\omega_1)\Delta\omega, \ldots$ is to adequately approximate the target spectral density function. Figure 2 shows an example where the frequency discretization is overly coarse. Secondly, the physical resolution Δx must be selected so that the spectral density above the frequency $2\pi/\Delta x$ is negligible. Failure to do so will result in an underestimation of the total variance of the process. In fact the FFT formulation given

above folds the power corresponding to frequencies between $\pi/\Delta x$ and $2\pi/\Delta x$ into the power at frequencies below the Nyquist limit $\pi/\Delta x$. This results in the point variance of the simulation being more accurate than if the power above the Nyquist limit were ignored, however it leads to a non-uniqueness in that a family of spectral density functions, all having the same value of $G(\omega_k)+G(\omega_{K-k})$, yield the same process. In general it is best to choose Δx so that the power above the Nyquist limit is negligible. The second term involving the symmetric frequency $G(\omega_{K-k})$ is included here because the point variance is the most important second-order characteristic.

Unfortunately, many applications dictate the size and discretization of the field *a-priori* or the user may want to have the freedom to easily consider other geometries or spectral density functions. Without a good deal of careful thought and analysis, the FFT approach can easily yield highly erroneous results.

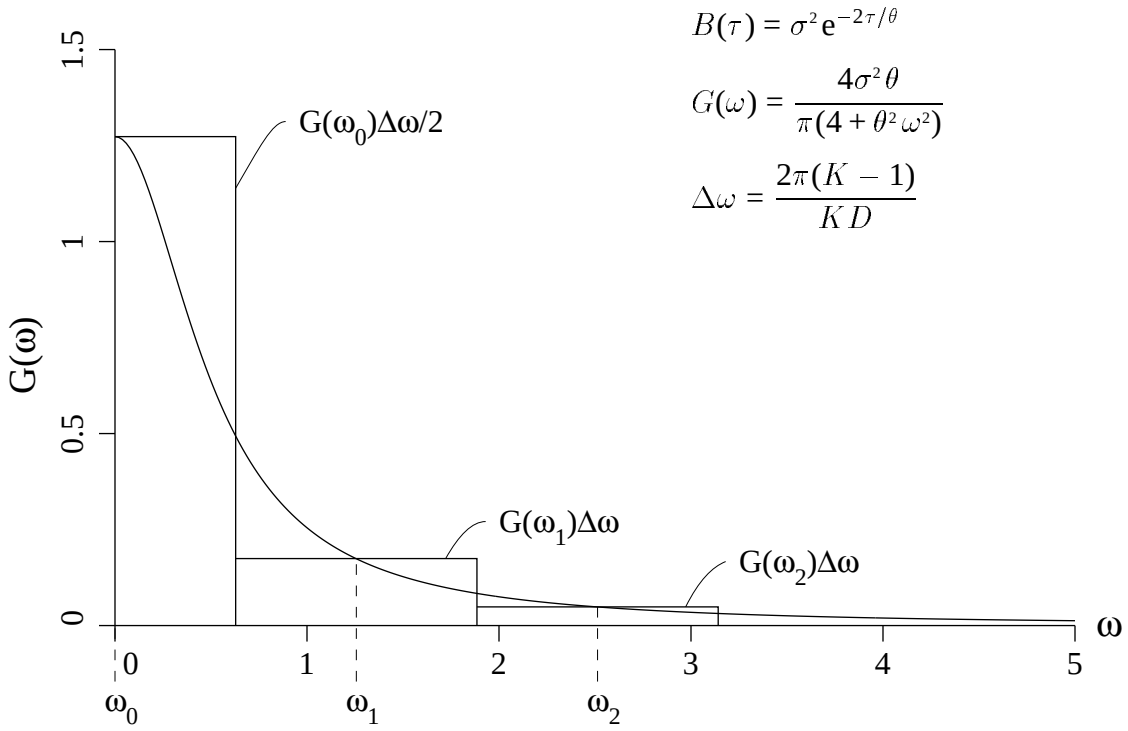

Figure 2 Example of overly coarse frequency discretization resulting in a poor estimation of point variance (D = 5 and θ = 4).

A major advantage of the FFT method is that it can easily handle anisotropic fields with no sacrifice in efficiency. The field need not be square, although many implementations of the FFT require the number of points in the field in any coordinate direction to be a power of two. Regarding efficiency, it should be pointed out that the time to generate the first realization of the field is generally much longer than that required to generate subsequent realizations. This is because the statistics of the Fourier coefficients must be calculated only once (see Eq.'s 15 and 16).

The Turning Bands Method

The Turning Bands Method (TBM), as originally suggested by Matheron (1973), involves the simulation of random fields in two- or higher-dimensional space by using a sequence of one-dimensional processes along lines crossing the domain. With reference to Figure 3, the algorithm can be described as follows,

1) choose an arbitrary origin within or near the domain of the field to be generated,
2) select a line i crossing the domain having a direction given by the unit vector $\underset{\sim}{u}_i$ which may be chosen either randomly or from some fixed set,
3) generate a realization of a one-dimensional process, $Z_i(\xi_i)$, along the line i having zero mean and covariance function $B_1(\tau_i)$ where ξ_i and τ_i are measured along line i,
4) orthogonally project each field point $\underset{\sim}{x}_k$ onto the line i to define the coordinate ξ_{ki} ($\xi_{ki} = \underset{\sim}{x}_k \cdot \underset{\sim}{u}_i$ in the case of a common origin) of the one-dimensional process value $Z_i(\xi_{ki})$,
5) add the component $Z_i(\xi_{ki})$ to the field value $Z(\underset{\sim}{x}_k)$ for each $\underset{\sim}{x}_k$,
6) return to step (2) and generate a new one-dimensional process along a subsequent line until L lines have been produced,
7) normalize the field $Z(\underset{\sim}{x}_k)$ by dividing through by the factor $\sqrt{L}$.

Essentially, the generating equation for the zero-mean discrete process $Z(\underset{\sim}{x})$ is given by

$$Z(\underset{\sim}{x}_k) = \frac{1}{\sqrt{L}} \sum_{i=1}^{L} Z_i(\underset{\sim}{x}_k \cdot \underset{\sim}{u}_i), \tag{30}$$

where if the origins of the lines and space are not common, the dot product must be replaced by some suitable transform. This formulation depends on knowledge of the one-dimensional covariance function, $B_1(\tau)$. Once this is known, the line processes can be produced using some efficient 1-D algorithm.

The covariance function $B_1(\tau)$ is chosen such that the multi-dimensional covariance structure $B_n(\underset{\sim}{\tau})$ in $\mathbb{R}^n$ is reflected over the ensemble. For two-dimensional isotropic processes, Mantoglou and Wilson (1981) give the following relationship between $B_2(\underset{\sim}{\tau})$ and $B_1(\eta)$ for $r = |\underset{\sim}{\tau}|$,

$$B_2(r) = \frac{2}{\pi} \int_0^r \frac{B_1(\eta)}{\sqrt{r^2 - \eta^2}}\, d\eta, \tag{31}$$

which is an integral equation to be solved for $B_1(\eta)$. In three dimensions, the relationship between the isotropic $B_3(r)$ and $B_1(\eta)$ is particularly simple,

$$B_1(\eta) = \frac{d}{d\eta}\Big(\eta\, B_3(\eta)\Big). \tag{32}$$

Mantoglou and Wilson supply explicit solutions for either the equivalent one-dimensional covariance function or the equivalent one-dimensional spectral density function for a variety of common multi-dimensional covariance structures.

In this implementation of the TBM, the line processes were constructed using a 1-D FFT algorithm as discussed in the previous section. The LAS method was not used for this purpose because

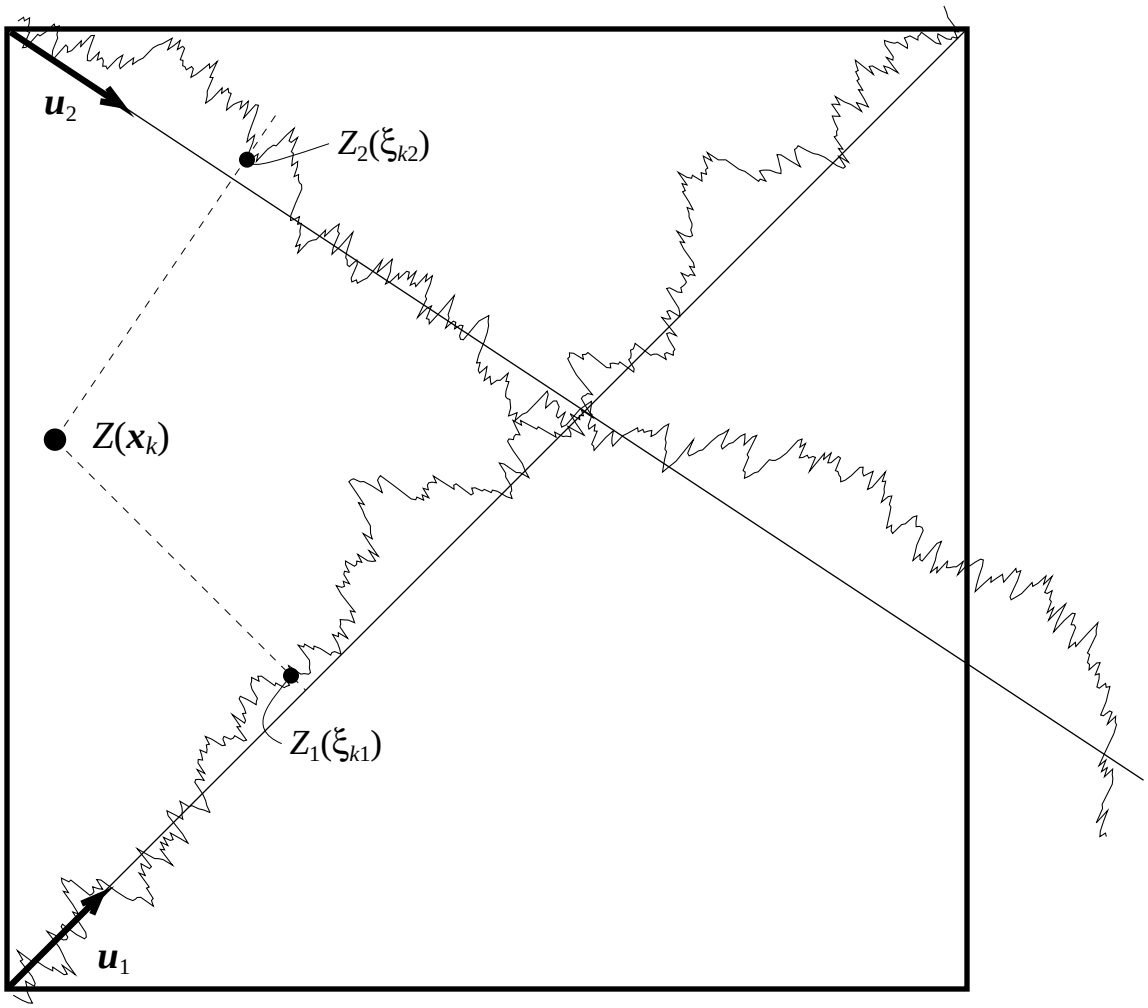

Figure 3. The Turning Bands Method: contributions from the line process $Z_i(\xi_i)$ at the closest point are summed into the field process $Z(\underset{\sim}{x})$ at $\underset{\sim}{x}_k$.

the local averaging introduced by the method would complicate the resulting covariance function of (31). Line lengths were chosen to be twice that of the field diagonal to avoid the symmetric covariance problem inherent with the FFT method. To reduce errors arising due to overly coarse discretization of the lines, the ratio between the incremental distance along the lines, $\Delta\xi$, and the minimum incremental distance in the field along any coordinate, Δx, was selected to be $\Delta\xi/\Delta x = \frac{1}{2}$.

Figure 4 represents a realization of a 2-D process. The finite number of lines used, in this case 16, results in a streaked appearance of the realization. A number of origin locations were experimented with to mitigate the streaking, the best appearing to be the use of all four corners as illustrated in Figure 3 and as used in Figure 4. The corner selected as an origin depends on which quadrant the unit vector $\underset{\sim}{u}_i$ points into. If one considers the spectral representation of the one-dimensional random processes along each line (see 2) it is apparent that the streaks are a result of constructive/destructive interference between randomly oriented traveling plane waves. The effect will be more pronounced for narrow band processes and for a small number of lines. For this particular covariance function (see 4), the streaks are still visible when 32 lines are used, but, as shown in Figure 5, are negligible when using 64 lines (the use of number of lines which are powers of 2 is arbitrary). While the 16

line case runs at about the same speed as the 2-D LAS approach, the elimination of the streaks in the realization comes at a price of running about 4 times slower. The streaks are only evident in an average over the ensemble if non-random line orientations are used, although they still appear in individual realizations in either case. Thus, with respect to each realization, there is no particular advantage to using random versus non-random line orientations.

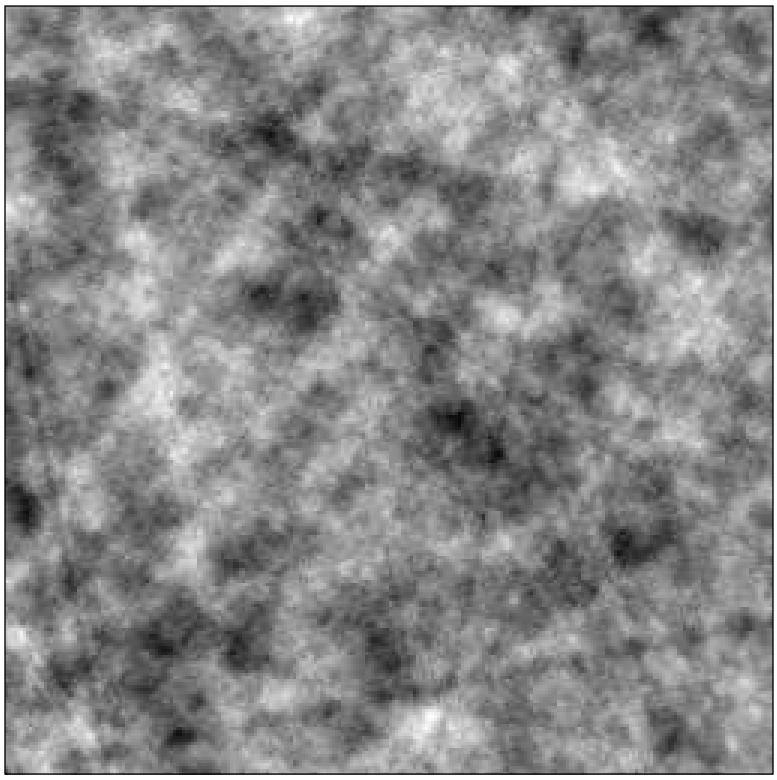

Figure 4. Sample function of a 2-D field via TBM using 16 lines.

Since the streaks are present in the field itself, this type of error is generally more serious than errors in the variance or covariance field. For example, if the field is being used to represent soil conductivity, then the streaks could represent paths of reduced resistance to flow, a feature which may not be desirable in a particular study. Crack propagation studies may also be very sensitive to such linear correlations in the field. For applications such as these, the Turning Bands method should only be used with a sufficiently large number of lines. This may require some preliminary investigation for arbitrary covariance functions. In addition, the minimum number of lines in 3 and higher dimensions is difficult to determine due to visualization problems.

Note that the Turning Bands Method does not suffer from the symmetric covariance structure that is inherent in the FFT approach. The variance field and covariance structure are also well preserved. However, the necessity of finding an equivalent 1-D covariance or spectral density function through an integral equation along with the streaked appearance of the realization when an insufficient number of lines are used makes the method less attractive. Using a larger number of lines, TBM is probably the most accurate of the three methods considered, at the expense of decreased efficiency. TBM can be extended to anisotropic fields, although there is an additional efficiency penalty associated with such an extension since the 1-D process statistics must be recalculated for each new line orientation (see Mantaglou and Wilson, 1981, for details).

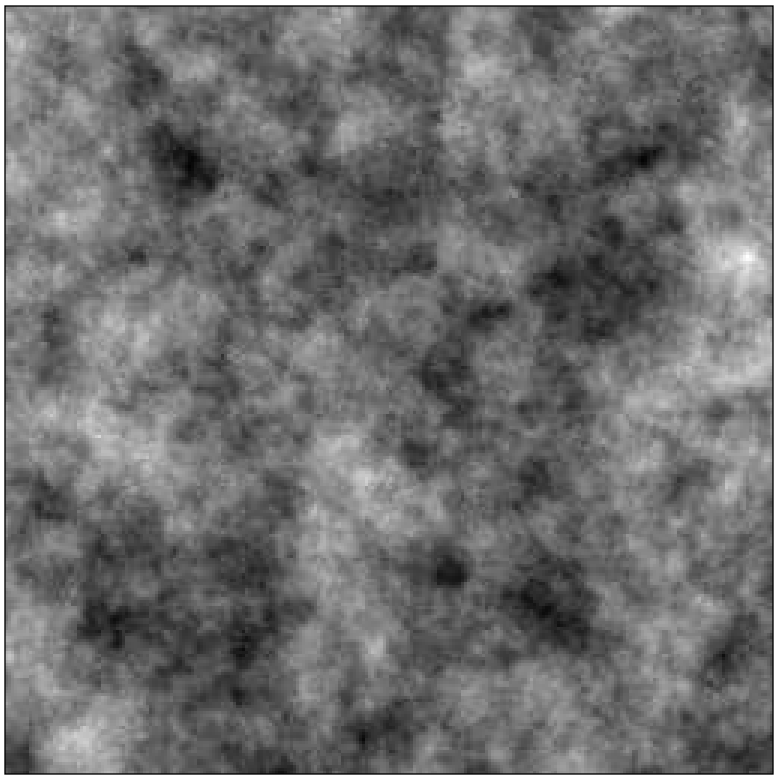

Figure 5. Sample function of a 2-D field via TBM using 64 lines.

The Local Average Subdivision Method

Of the three methods considered, the LAS method is probably the most difficult to implement. The details are given by Fenton and Vanmarcke (1990). The one- and two-dimensional implementation of LAS used for this study differs slightly from that reported by Fenton and Vanmarcke in that an initial set of cells are generated directly from the associated covariance matrix according to Eq. 3. Specifically, in the 1-D case, a positive integer k_1 is found so that the total number of cells, N_1, desired in the final field can be expressed as

$$N_1 = k_1(2^m) \tag{33}$$

where m is the number of subdivisions to perform and k_1 is as large as possible with $k_1 \leq 16$. In one-dimension, this modification was implemented to reduce the variance field errors discussed later. In two dimensions, two positive integers k_1 and k_2 are found such that $k_1 k_2 \leq 256$ and the field dimensions can be expressed as

$$N_1 = k_1(2^m) \tag{34a}$$

$$N_2 = k_2(2^m) \tag{34b}$$

from which the first $k_1 \times k_2$ lattice of cell values are simulated directly using covariance matrix decomposition (3). Since the number of subdivisions, m, is common to the two parameters, one is not entirely free to choose N_1 and N_2 arbitrarily. It does, however, give a reasonable amount of discretion in generating non-square fields, as is also possible with both the FFT and TBM methods.

Perhaps the major advantage of the LAS method is that it produces a field of local average cells whose statistics are consistent with the field resolution. As such, it is well suited to problems where the system is represented by a set of elements and average properties over each element are desired. Changing the element size automatically results in changes in the statistics of the element average, as dictated by random field theory. This is appealing since almost all measured engineering properties are based on local averages (concrete strength, for example, is based on a finite volume cylinder).

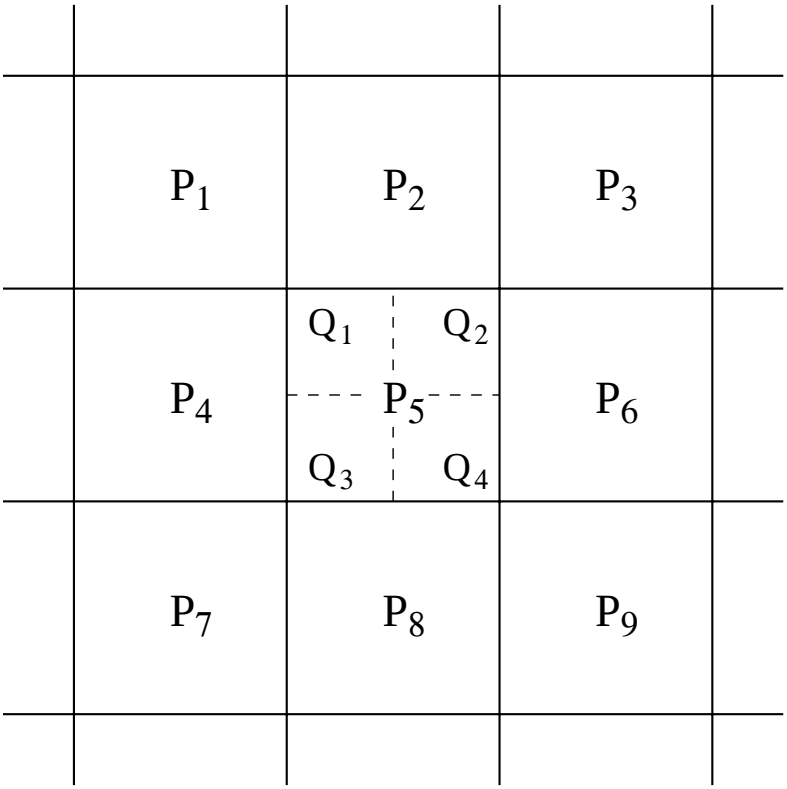

Figure 6. Local Average Subdivision in two-dimensions.

To enable a discussion of some of the features and problems with the LAS method, a brief overview of the 2-D implementation will be repeated here. The 2-D LAS method involves a subdivision process in which a 'parent' cell is divided into 4 equal sized cells. In Figure 6, the parent cells are denoted P_i, $i = 1, 2, \ldots$ and the subdivided, or child cells are denoted Q_j, $j = 1, 2, 3, 4$. Although each parent cell is eventually subdivided in the LAS process, only P_5 is subdivided in Figure 6 for simplicity. Using vector notation, the values of $\underset{\sim}{Q}^T = \{Q_1, Q_2, Q_3, Q_4\}$ are obtained by adding a mean term to a random component. The mean term derives from a best linear unbiased estimate using a 3×3 neighborhood of the parent values, in this case $\underset{\sim}{P}^T = \{P_1, \ldots, P_9\}$. Specifically

$$\underset{\sim}{Q} = \underset{\approx}{A}^T \underset{\sim}{P} + \underset{\approx}{C} \underset{\sim}{U} \tag{35}$$

where $\underset{\sim}{U}$ is a random vector with independent $N(0, 1)$ elements. This is essentially an ARMA model in which the 'past' is represented by the previous coarser resolution stages. Defining the covariance matrices

$$\underset{\approx}{R} = \mathrm{E}\left[\underset{\sim}{P}\underset{\sim}{P}^T\right], \tag{36a}$$

$$\underset{\sim}{S} = \mathrm{E}\left[\underset{\sim}{P}\underset{\sim}{Q}^T\right], \quad \text{and} \tag{36b}$$

$$\underset{\sim}{B} = \mathrm{E}\left[\underset{\sim}{Q}\underset{\sim}{Q}^T\right], \tag{36c}$$

then the matrix $\underset{\sim}{A}$ is determined by

$$\underset{\sim}{A} = \underset{\sim}{R}^{-1}\,\underset{\sim}{S} \tag{37}$$

while the lower triangular matrix $\underset{\sim}{C}$ satisfies

$$\underset{\sim}{C}\,\underset{\sim}{C}^T = \underset{\sim}{B} - \underset{\sim}{S}^T\underset{\sim}{A} \tag{38}$$

Note that the matrix on the right hand side of (38) is only rank 3, so that the 4×4 matrix $\underset{\sim}{C}$ has a special form with columns summing to zero (thus $C_{44} = 0$). While this results from the fact that all the expectations used in Eq.'s (36) are derived using local average theory over the cell domains, the physical interpretation is that upwards averaging is preserved, ie. that $P_5 = \frac{1}{4}(Q_1 + Q_2 + Q_3 + Q_4)$. This means that one of the elements of $\underset{\sim}{Q}$ is explicitly determined once the other three are known.

Although Figure 1 illustrates the superior performance of the LAS method over the FFT method in one dimension, a systematic bias in the variance field is observed in two dimensions. Figure 7 shows a grey scale image of the estimated cell variance in a two-dimensional field obtained by averaging over the ensemble. There is a definite pattern in the variance field – the variance tends to be lower near the major cell divisions, that is at the $1/2$, $1/4$, $1/8$, etc. points of the field. This is because the actual diagonal, or variance, terms of the 4×4 covariance matrix corresponding to a subdivided cell are affected by the truncation of the parent cell influence to a 3×3 neighborhood. The error in the variance is compounded at each subdivision stage and cells close to 'older' cell divisions show more error than do 'interior' cells. The magnitude of this error varies with the number of subdivisions, the scale of fluctuation, and type of covariance function governing the process and can be obtained by evaluating the transfer function of Eq. (35). Such a quantitative analysis is yet to be performed.

Figure 8 depicts the estimated variances along a line through the plane for both the LAS and TBM methods. Along this line, the pattern in the LAS estimated variance is not particularly noticeable and the values are about what would be expected for an estimate over the ensemble. Figure 9 compares the estimated covariance structure in the vertical and horizontal directions, again for the TBM (64 lines) and LAS methods. In this respect, both the LAS and the TBM methods are reasonably accurate. In addition, the LAS method yields good quality realizations and an accurate mean field.

The LAS method can be used to produce anisotropic random fields with no code change and no loss in efficiency, however the anisotropic nature of such a field is due entirely to the initial production of a $k_1 \times k_2$ field via covariance matrix decomposition. The subdivision algorithm itself is incapable of preserving anisotropy, the directional scales of fluctuation tending toward the minimum for the field. Thus, although the field may be globally anisotropic, small neighborhoods of cells at the final resolution tend to follow an isotropic correlation structure. One notes that ellipsoidally anisotropic random fields can always be produced from isotropic random fields by suitably stretching the coordinate axes and so this error is not always a problem.

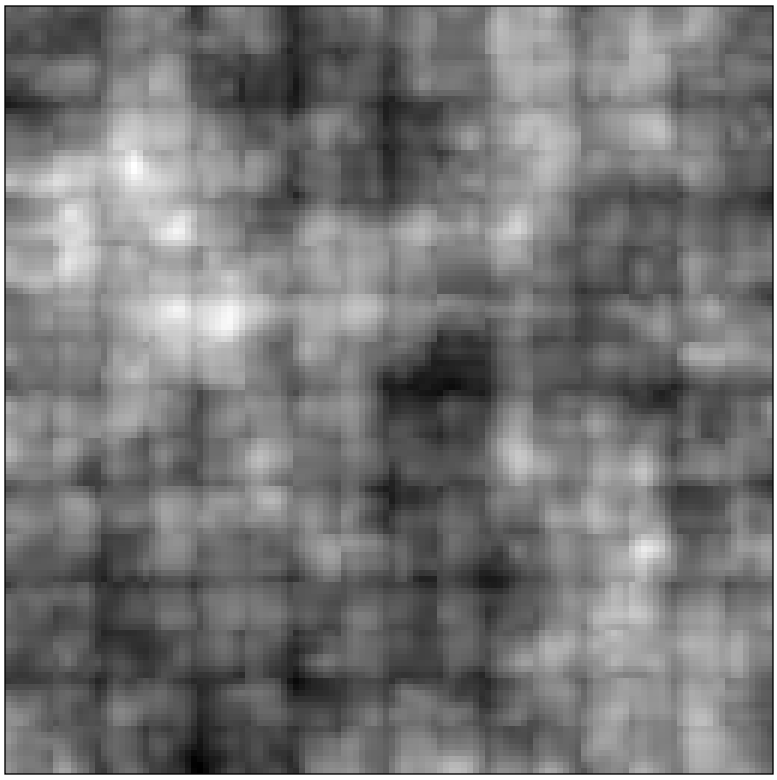

Figure 7. Two-dimensional LAS variance field estimated over 200 realizations.

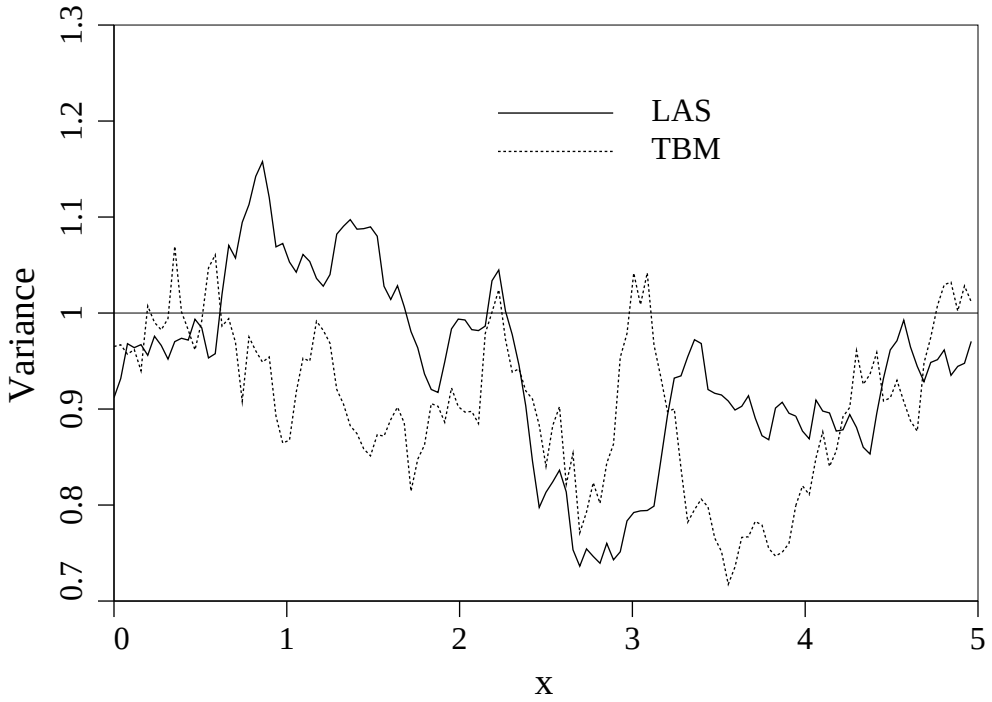

Figure 8. Variance along a horizontal line through the two-dimensional LAS and TBM fields estimated over 200 realizations.

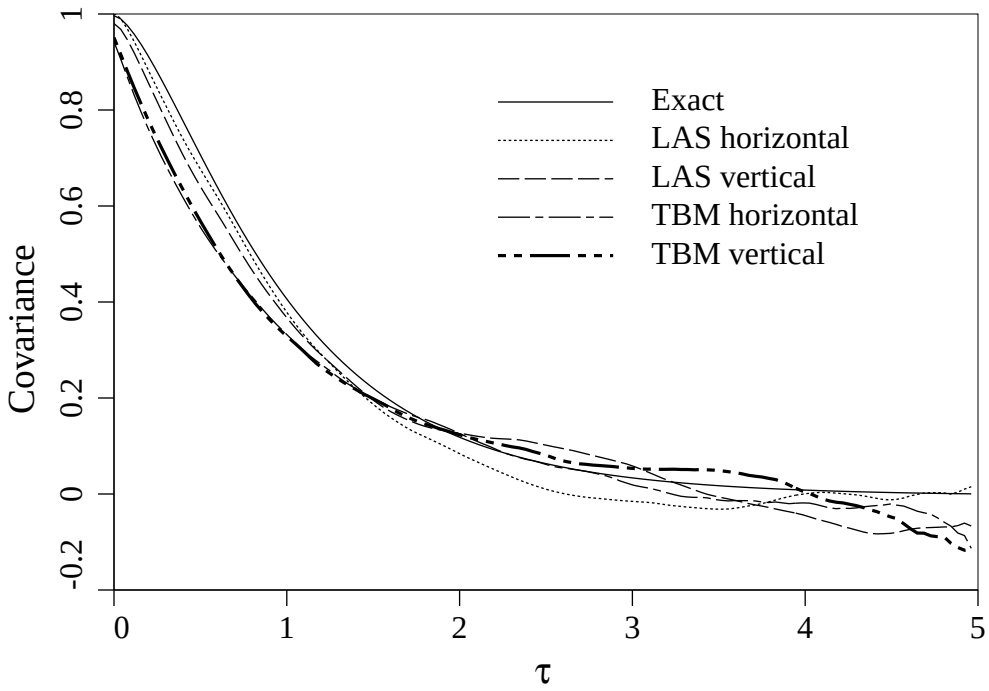

Figure 9. Covariance structure of the LAS and TBM two-dimensional random fields estimated over 200 realizations.

It may be possible to improve the LAS covariance approximations by extending the size of the parent cell neighborhood. A 3×3 neighborhood is used in the current implementation of the 2-D LAS algorithm, as shown in Figure 6, but any odd sized neighborhood could be used to condition the statistics of the subdivided cells. Larger neighborhoods have not been tested in two and higher dimensions, although in one dimension increasing the neighborhood size to 5 cells resulted in a more accurate covariance function representation, as would be expected.

The LAS method also depends on knowledge of the variance function which governs the variance reduction when a process is locally averaged. Although this function can be obtained through a direct, possibly numerical, integration of the covariance function, analytically exact variance functions can be difficult to find for some covariance functions in higher dimensions. Vanmarcke (1984) has derived the variance functions for a number of common random processes.

Comparison and Conclusions

The choice of a random field generator to be used for a particular problem or in general depends on many issues. Table 1 shows the relative run times of the three algorithms to produce identically sized fields. The times have been normalized with respect to the FFT method so that a value of 2 indicates that the method took twice as long. If efficiency alone were the selection criteria, then either the TBM with a small number of lines or the LAS methods would be selected, with probably the LAS a better choice if streaking is not desired. However, efficiency of the random field generator is often not an overriding concern – in many applications, the time taken to generate the field is dwarfed by the time taken to subsequently process or analyze the field. Substantial changes in generator efficiency may be hardly noticed by the user.

Table 1. Comparison of run-times of the FFT, TBM and LAS algorithms in one and two-dimensions.

Dimension	FFT	LAS	TBM	
			16 lines	64 lines
1-D	1.0	0.70	–	–
2-D	1.0	0.55	0.64	2.6

As a further comparison of the accuracy of the FFT, TBM, and LAS methods, a set of 200 realizations of a 128×128 random field were generated using the Gauss-Markov covariance function with a scale of fluctuation $\theta = 2$ and a physical field size of 5×5. The mean and variance fields were calculated by estimating these quantities at each point in the field (averaging over the ensemble) for each algorithm. The upper and lower 90% quantiles are listed in Table 2 along with those predicted by theory assuming a normal distribution. To obtain these numbers, the mean and variance fields were first estimated, then upper and lower bounds were found such that 5% of the field exceeded the bounds above and below, respectively. Thus 90% of the field is observed to lie between the bounds. It can be seen that all three methods yield very good results with respect to the expected mean and variance quantiles. The TBM results were obtained using 64 lines. Although these results are strictly only valid for the particular covariance function used, they are believed to be generally true over a wider variety of covariance functions and scales of fluctuation.

Table 2. Upper and lower 90% quantiles of the estimated mean and variance fields for the FFT, TBM, and LAS methods (200 realizations).

Algorithm	Mean	Variance
FFT	$(-0.06, 0.12)$	$(0.87, 1.19)$
TBM	$(-0.11, 0.06)$	$(0.83, 1.14)$
LAS	$(-0.12, 0.09)$	$(0.82, 1.13)$
Theory	$(-0.12, 0.12)$	$(0.84, 1.17)$

Purely on the basis of accuracy in the mean, variance and covariance structures, the best algorithm of those consider here is probably the TBM method using a large number of lines. The TBM method is also one of the easiest to implement once an accurate 1-D generator has been implemented. Unfortunately, there is no clear rule regarding the minimum number of lines to be used to avoid streaking. In two dimensions using the Gauss-Markov covariance function, it appears that at least 50 lines should be employed. However, as mentioned, narrow band processes may require more. In three dimensions, no such statements can be made due to the difficulty in studying the streaking phenomena off a plane. Presumably one could use a 'density' of lines similar to that used in the two-dimensional case, perhaps subtending similar angles, as a guide. The TBM method is reasonably easy to use in practice as long as the equivalent 1-D covariance or spectral density function can be found.

The FFT method suffers from symmetry in the covariance structure of the realizations. This can be overcome by generating fields twice as large as required in each coordinate direction and ignoring the surplus. This correction results in slower run times (a factor of 2 in 1-D, 4 in 2-D, etc.). The FFT method is also relatively easy to implement and the algorithm is similar in any dimension. Its ability to easily handle anisotropic fields makes it the best choice for such problems. Care must be taken when selecting the physical field dimension and discretization interval to ensure that the spectral density function is adequately approximated. This latter issue makes the method more difficult to use in practice. However, the fact that the FFT approach employs the spectral density function directly makes it an intuitively attractive method, particularly in time dependent applications.

The LAS method has a systematic bias in the variance field, in two and higher dimensions, which is not solvable without changing the algorithm. However, the error generally does not result in values of variance that lie outside what would be expected from theory – it is primarily the pattern of the variance field which is of concern. Of the three methods considered, the LAS method is the most difficult to implement and it depends on the variance function representation of the field. It is, however, one of the easiest to use once coded since it requires no decisions regarding its parameters, and it is generally the most efficient. If the problem at hand requires or would benefit from a local average representation, then the LAS method is the logical choice.

Acknowledgements

The author would like to thank the Natural Sciences and Engineering Research Council of Canada for their financial support under Grant OPG0105445. Any opinions, findings, and conclusions and recommendations are those of the author and do not necessarily reflect the views of the aforementioned organization.

Appendix I. References

Cooley, J. W. and Tukey, J. W. (1965). "An Algorithm for the Machine Calculation of Complex Fourier Series," *Mathematics of Computation*, **19**(90), 297-301.

Fenton, G. A. and Vanmarcke, E. H. (1990). "Simulation of Random Fields via Local Average Subdivision," *ASCE J. Engrg. Mech.*, **116**(8), 1733–1749.

Fenton, G.A. (1990). "Simulation and Analysis of Random Fields," Ph.D. Thesis, Princeton University, Princeton, New Jersey.

Mantoglou, A. and Wilson, J. L. (1981). "Simulation of Random Fields with the Turning Bands Method" , MIT, Dept. Civil Engrg., Report #264, Cambridge, MA.

Matheron, G. (1973). "The Intrinsic Random Functions and their Applications," *Adv. in Appl. Probab.*, **5**, 439-468.

Mignolet, M.P. and Spanos, P.D. (1992). "Simulation of homogeneous two-dimensional random fields: Part I – AR and ARMA Models," *ASME J. Appl. Mech.*, **59**, S260–S269.

Shinozuka, M. and Jan, C. M. (1972). "Digital Simulation of Random Processes and it Applications," *J. Sound Vibration*, **25**(1), 111-128.

Spanos, P.D. and Mignolet, M.P. (1992). "Simulation of homogeneous two-dimensional random fields: Part II – MA and ARMA Models," *ASME J. Appl. Mech.*, **59**, S270–S277.

Vanmarcke, E. H. (1984). *Random Fields: Analysis and Synthesis*, The MIT Press, Cambridge, Massachusetts, .

Yaglom, A. M. (1962). *An Introduction to the Theory of Stationary Random Functions*, Dover, Mineola, NY, .

Appendix II. Notation

The following symbols are used in this paper:

$\mathcal{A}_k$ = Fourier coefficient (real part)

$\mathcal{B}_k$ = Fourier coefficient (imaginary part)

$B(\cdot)$ = covariance function

$\hat{B}$ = algorithmic covariance function

$\underset{\approx}{B}$ = covariance matrix

$\mathcal{C}_k$ = random amplitude

D = physical dimension of the field

E $[\cdot]$ = expectation operator

f = weighting function

$G(\cdot)$ = one-sided spectral density function

i = square root of negative one

K = number of frequency and spatial points

$\underset{\approx}{L}$ = lower triangular matrix

N = number of spatial points

$\underset{\sim}{P}$ = vector of parent cell values (LAS)

$\underset{\sim}{Q}$ = vector of child cell values (LAS)

$S(\cdot)$ = two-sided spectral density function

$\underset{\sim}{U}$ = vector of independent random numbers

W = white noise process

$\mathcal{X}_k$ = complex Fourier coefficient

$\underset{\sim}{x}$ = spatial coordinate

Z = random field

$\underset{\sim}{Z}$ = vector of random field values at discrete points or cells

Φ_k = random phase angle

θ = scale of fluctuation

σ = standard deviation

$\underset{\sim}{\tau}$ = lag vector

$\underset{\sim}{\omega}$ = frequency